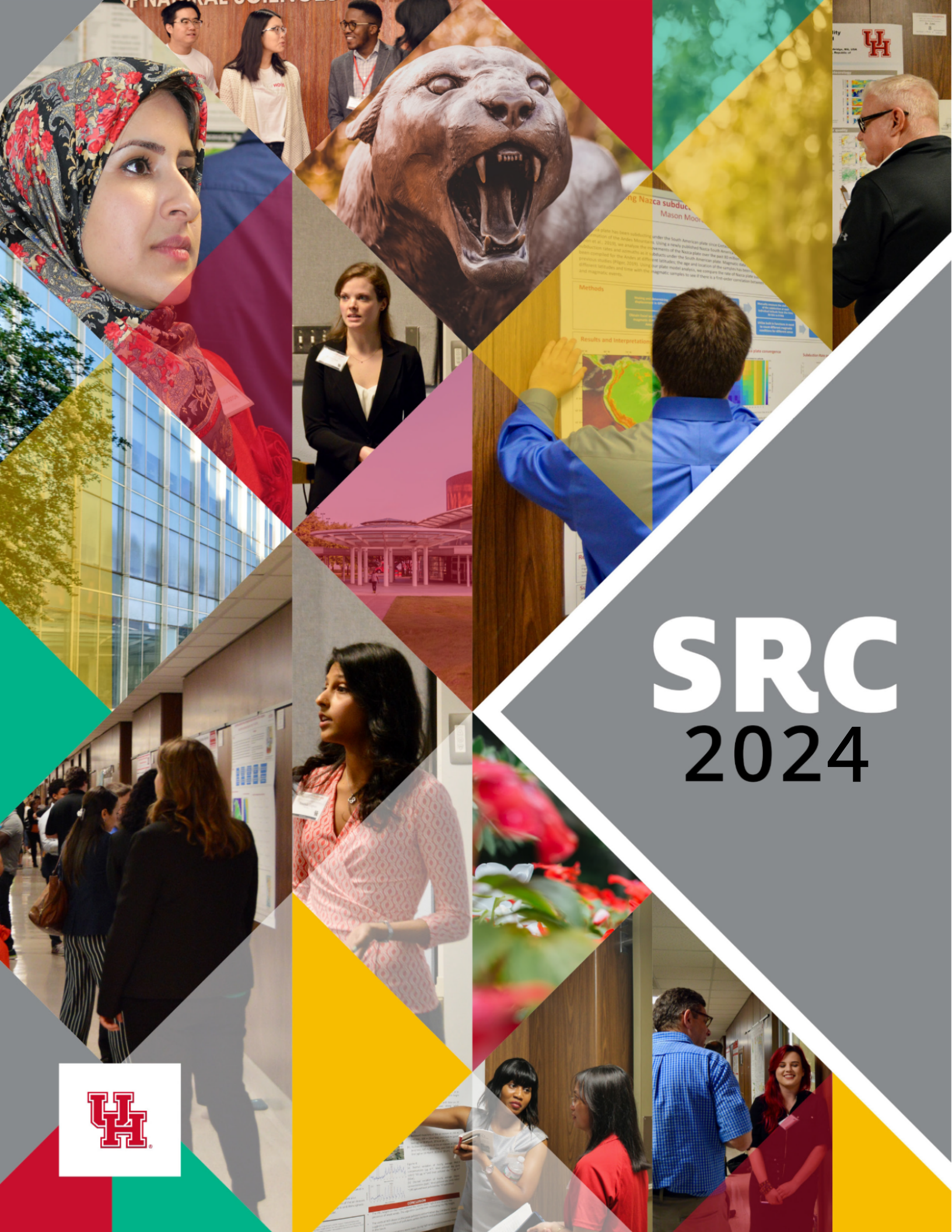

SRC
2024

University of Houston

Earth and Atmospheric Sciences

37th Annual Student Research Conference

Friday, April 26th, 2024

Table of Contents

American Association of Petroleum Geologists (AAPG)
aapg.wildcatters@gmail.com

American Meteorological Society (AMS)
uhstudentams@gmail.com

Association of Environmental and Engineering Geologists (AEG) and American Institute of Professional Geologists (AIPG)
AEGatUH2@gmail.com

Geological Society (GeoSociety)
geosocietyatuh@gmail.com

Society of Exploration Geophysicists (SEG) Wavelets
segwavelets@gmail.com

Schedule

Check-In & Breakfast	8:30 - 9:30 a.m.
Oral Presentations	9:30 - 10:30 a.m.
Coffee Break	10:30 - 11:00 a.m.
Oral Presentations	11:00 - 12:00 p.m.
Lunch Break	12:00 - 1:00 p.m.
Poster Presentations & Lab Open House	1:00 - 3:00 p.m.
Coffee Break	3:00 - 3:30 p.m.
Awards Ceremony	3:30 - 4:30 p.m.
Group Photo	4:30 p.m.
Happy Hour	5:00 - 7:30 p.m.

Oral Presentations

SR1 223

9:30 a.m.

Abdolrazzagh Javid

Testing Gassmann's Undrained Bulk Modulus using Effective Elastic Media Approaches

9:45 a.m.

Lucille Baker-Stahl

Deltaic Implications from the Rheology of Freezing Sediment

10:00 a.m.

Jumoke Akinpelu

Re-defining the continent-ocean boundary beneath the distal Niger delta and expanding its deepwater, hydrocarbon play fairway based on the wider zone of continental rifts and syn-rift source rocks.

10:15 a.m.

Mayra D. L. Carrasquilla

Seismic Anisotropy of Granitic Rocks from a Fracture Stimulation Well at Utah FORGE Using Ultrasonic Measurements

Oral Presentations

SR1 223

11:00 a.m.

Asmara Lehrmann

Fingerprinting paleoenvironments offshore Thwaites Glacier with modern foraminifera

11:15 a.m.

Md Upal Shahriar

Crustal structure and tectonostratigraphy of the Andaman oblique-subduction margin and its control on hydrocarbon potential

11:30 a.m.

Amna Afzal

Quantification and Primary Source Analysis of Per- and Polyfluoroalkyl Substances (PFAS) in Edwards Aquifer and Neches River - Southern Texas

11:45 a.m.

Arya Tilak

Distribution, Age, and Significance of Cretaceous-Paleogene Intertrappean Beds in the Deccan Volcanic Province, India

Oral Presentations

SR1 634

9:30 a.m.

Karissa Vermillon

Resurrecting Rodinia: Who was our western neighbor?

9:45 a.m.

Divine Kalu

Mapping the Unknown: A Tale of Mineral Exploration, Inversion and Marvel of Invertible Neural Networks

10:00 a.m.

Joe McNease

Surface wave workflows for the Texas Gulf Coast

Oral Presentations

SR1 634

11:00 a.m.

Fnu Anshika

Development of an Analytical Method to determine of Airborne Phthalates

11:15 a.m.

Mahmoudreza Momeni

Development of a Python-based Data Assimilation Framework (PyDAF)

11:30 a.m.

Anvesha Subramanian

A Novel Nanocarbon Infused Gum Arabic Sensing Skin Optimized for On-Skin Electronics and Temporary E-Tattoos

11:45 a.m.

Kenneth Shipper

Flexural, crustal, and basin modeling of the Jurassic volcanic-clastic transition along the Guyana-Suriname margin

Poster Presentations

Energy & Earth Resources

Ruth Beltran
Aptian-Albian tectonic evolution of a hyperextended, continental rift system and its transition into oceanic crust in the ultra-deepwater Campos basin, Brazil

Daniel Maya
Using gravity modeling to constrain the crustal structure of the Early Cretaceous volcanic-rifted margin of Uruguay

Tessa Heaton
A Multifaceted Geochemical Study on Hydrocarbons and Energy Transition Avenues of the Bonaparte Basin, NW Australia

Mohammad Jahirul Alam
Investigating the Complexities of VOC Sources in Mexico City in the Years 2016–2022

Mohammad Younas
Geospatial analytics of driving mechanism of land subsidence in Gulf Coast of Texas, United States

Poster Presentations

Earth & Planetary Dynamics

Johanna Villagomez
Monitoring ground motions caused by possible shore fault movement and ocean waves

Presley Greer
Detecting subsurface ice wedges using GPR at the CRREL Permafrost Tunnel in Fox, Alaska

Mikaela Garcia
Quantifying Erosion at Sargent Beach, Texas Using Remote Sensing

Joshua Miller
Paleogene arc collision and migration in the Bering Sea interpreted from regional magnetic and gravity data

Jennifer Welch
Unveiling the Hidden Threat: Drought-Induced Inelastic Subsidence in Expansive Soils

Muhammad Asif
Improving InSAR Measurements: The Role of High-Resolution LIDAR DEMs in Topographic Correction

Kaitlyn Bryant
Using a compilation of vintage seismic reflection data and earthquake data to understand the tectonic origin of the Puerto Rico-Virgin Islands Arch

Poster Presentations

Atmospheric & Earth Surface Systems

Samantha Baker
Temporary Sediment Storage in Proglacial Lakes Near Kangerlussuaq, Greenland

Sagar Rawak
Use of GPS to study the Land Subsidence and it's effects in Harris County

M. Ahmad
Machine learning models for an Ozone Episode in Mexico City

Kennedy Potter
Subaqueous Carbon Sequestration in Elephant Butte Reservoir, New Mexico

Caroline Mandujano
Investigating Downstream Fining in Kangerlussuaq, Greenland

Leo Collier
Monitoring Seaward Dune Recovery on Matagorda Peninsula

Alejandro Aguilar
Unraveling the Subsurface Story: Investigating Fluvial Sedimentology of the Rio Grande Using Ground Penetrating Radar

Irfan Karim
Investigating the anthropogenic sources: Methane and Carbon Dioxide Emissions in Houston, Texas

Jincheol Park
First Top-Down Diurnal Updates to NOx Emissions Inventory in Asia Informed by the Geostationary Environment Monitoring Spectrometer (GEMS) Tropospheric NO2 Columns

Poster Presentations

Atmospheric & Earth Surface Systems

Xinyue Wang
Global Energy Imbalance of Saturn

Thishan D Karandana
Impact of California Wildfires on Atmospheric Trace Gases

Daniel Ragusa
Tracking the water pH and atmospheric CO2 evolution during synthetic carbonate precipitation

Nilay Gungor
Proglacial Delta-Front Sediment Transport in West Greenland

Sarah Garcia
Carbon Emission as a Consequence of High Sedimentation and Drought at Elephant Butte Reservoir, New Mexico

Lab Open House

Rock Physics Lab (RPL)

Location: SR1, Rooms 104-108, B-8
Lab hosts: Dr. Yingcai Zheng

RPL is a research lab to conduct world class research on Seismic Rock Physics. Based on our 25+ years' experiments and achievements on seismic rock physics and collaboration with industry through the Fluids/DHI Consortium, we have been focusing on energy transition, especially on GCS and geothermal. From lab data measurement, model development, to application software, we use integrated research strategies of combining the fluid and rock properties to provide academic results and industry solutions. The lab research focuses on:

1. Seismic properties of hydrocarbon fluids at in-situ conditions and rocks from conventional reservoirs (sands, sandstone, tight gas sands and carbonates);
2. All kinds of rocks and fluids from unconventional reservoirs: oil shale, shale gas, shale oil, coal, gas hydrate, and heavy oil sands;
3. Rock parameters, seismic velocities, modulus, including rock mechanics and LF measurements;
4. Experimental and theoretical investigation on poro-elasticity (including digital rock modeling), velocity dispersion, wave attenuation, elastic anisotropy, fractured reservoir, static and dynamic elasticity;
5. Seismic attributes as direct hydrocarbon indicator (DHI), reservoir delineation, 4-D seismic monitoring, manage unconventional reservoirs;
6. Physical and seismic properties of rocks and fluids related to energy transitions: GCS and geothermal;
7. Training graduate students.

Benson-Lamarr Thermal Ionization Mass Spectrometry Lab

Location: SR1, Rooms 321 & 325
Lab hosts: Dr. Michael Antonelli and Morgann Farley

The Benson-Lamarr Thermal Ionization Mass Spectrometry Lab (Rm 325 and 321)
This lab hosts two Thermoscientific Triton Mass Spectrometers: a Triton XT (aka 'George Benson') and a Triton Plus (aka 'Hedy Lamarr'). The lab also includes an associated clean lab for preparing samples for isotopic measurements by TIMS. With these instruments, we can perform radiogenic isotope measurements (for absolute age dating) and stable isotope measurements (for determining the conditions, mechanisms, and durations of natural chemical reactions that occured in Earth's geologic past). The lab specializes in the isotopic measurement of calcium, which has both radiogenic and stable isotope components, making it a particularly useful system for geochemistry. The lab also measures Sr, Nd, and other isotopic systems.

Lab Open House

Physical Sedimentology Lab

Location: SR1, Room 303

Lab hosts: Ariam Deleon, Jamie Jetton, Bridgette Kennedy, Margaret Sauer

The sedimentology lab at UH includes a Cilas 1190 laser particle size analyzer for sizing particles from 0.04 to 2,500 μm. The Cilas is integrated with an additional system for capturing particle images and analyzing various shape factors. The lab is also equipped with a Canberra germanium well-detector for gamma-ray spectroscopy. The system is designed for small volume samples and is used primarily for 210Pb and 137Cs measurement of recent sediments but is available for other gamma-ray measurements.

The lab has other standard equipment for working with sediments and sedimentary rocks, including a sonic bath, centrifuge, oven, sieves, and various microscopes. Computers in the lab are equipped with multibeam swath bathymetry processing software, seismic interpretation software, and log-correlation packages for integration of geophysical data with sample information.

Abstracts

Oral Presentations - SR1 223

Abdolrazzagh Javid

Testing Gassmann's Undrained Bulk Modulus using Effective Elastic Media Approaches

Originally developed in 1951, Gassmann's equations remain widely utilized in applied geophysics, particularly in fluid substitution. This equation enables the calculation of bulk modulus for fully saturated rocks based on parameters such as frame bulk modulus, porosity, fluid bulk modulus, and bulk modulus of solid grains. However, Thomsen (2023) has raised concerns about a logical error in the derivation of Gassmann's equations. To test the reliability of Gassmann's undrained bulk modulus, various theoretical approaches are explored, including Hashin–Shtrikman–Walpole Bounds, Voigt–Reuss Moduli, the Glinsky - DiMartini floating grain model, Berryman's equations for spherical, needle, and disc inclusions, and the Toksöz formulation for penny shaped cracks, as well as the O'Connell and Budiansky Self-Consistent Approximation for interacting pores. For most of these scenarios, including alternating fine layers of these with different porosities, the Gassmann's undrained bulk modulus for the effective medium is in numerical agreement with these exact theoretical models. Analytical solutions for Voigt-Reuss and Hashin-Shtrikman bounds show exact agreement. However, as pointed out by Thomsen, the Gassmann prediction disagrees with the Küster and Toksöz formulation for dilute concentrations of penny-shaped cracks. On the other hand, also for penny-shaped cracks, Gassmann is in good numerical agreement with the O'Connell-Budiansky self-consistent method for porosities equal to or less than the aspect ratio. This leads to the following hypotheses that remain to be investigated: (1) Gassmann's unproven use of Love's theorem pointed out by Thomsen may in fact be correct in some cases, possibly leading to a generalization for its use, (2) the Küster and Toksöz use of crack concentrations less than the aspect ratio as being dilute, being a geometric rather than a physical argument (the requirement that cracks not intersect), may in fact be too generous, with only much smaller concentrations agreeing with Gassmann, and with pore interactions possibly being important for larger concentrations than previously thought, and (3) the O'Connell-Budiansky self-consistent method of accounting for pore interaction, being heuristic rather than theoretically derived, may be a good approximation for crack concentrations less than or equal to the aspect ratio. However, disagreement with Gassmann's equation for larger concentrations suggests that it should be used with care.

Lucille Baker-Stahl

Deltaic Implications from the Rheology of Freezing Sediment

Deltas in Southwest Greenland are rapidly prograding in response to changes in Earth's atmospheric temperature leading to an increase in sediment-laden glacial runoff. Though Greenlandic delta topsets are well studied, the delta front and deep water sedimentation remain a missing link. It is, therefore, not possible at present to accurately quantify sediment partitioning in these systems without a better understanding of subaqueous sediment transport. We focus on the Quinnguata Kuusua River (or Watson River) in Kangerlussuaq, Greenland, which forms a delta with frequent avulsions and delta lip failures. The fluvial system is controlled by atmospheric temperature, with glacial meltwater discharge at temperatures above 0 °C and waning flow to ice cover at lower temperatures. During the warm season, high sediment discharge generates rapid deposition at active channel mouths which are the sites of previous delta lip failures. We investigate changes in the rheology of delta lip sediment in order to explain the continual reworking of the delta front. This is driven by the intensity of deposition and the extreme climatic shifts in the system leading to varied freeze-thaw and compaction processes. Sediment rheology in the laboratory is used to quantify changes in rheology across a range of temperature, pressure, and saturation conditions corresponding to the delta environment. Lab rheology experiments consist of consolidation and shear loading protocols in frozen, freeze-thawed, and unfrozen conditions. This is combined with a field derived sediment distribution model of the Kangerlussuaq delta from advection and diffusion. Results suggest that the timing and sequence of consolidation and freeze-thaw processes have a significant effect on fine grained sediment strength. We aim to understand how sediment conditions at the time of freezing–the consolidation that ensues, and the rate and timing of freeze-thaw processes–control the evolution of sediment strength and delta lip morphodynamics.

Abstracts

Oral Presentations - SR1 223

Jumoke Akinpelu

Re-defining the continent-ocean boundary beneath the distal Niger delta and expanding its deepwater, hydrocarbon play fairway based on the wider zone of continental rifts and syn-rift source rocks

The Niger Delta basin is an established and prolific hydrocarbon province based on a century of exploration and production of Cenozoic plays located on the inland delta, shelf, and slope. Progress in understanding the deeper, Cretaceous-sourced hydrocarbon plays in the deeper-water areas of the Niger Delta has been slower because of the lack of deeply-penetrating seismic reflection data integrated with gravity and magnetic data. In this study, I integrate seismic reflection, magnetic, and gravity data to expand the zone of Aptian-Albian continental rifting by a distance of 125 km in the seaward direction This expansion of the zone of continental rifting expands the exploration play fairway for rift-sourced hydrocarbons that are the source of recent, large discoveries to the west and southeast of the Niger Delta.

Interpretation of the study area's magnetic data shows northeast-southwest trending fracture zones and orthogonal spreading fabric in the post-Albian oceanic crust. This Cretaceous oceanic spreading fabric trends at right angles to a northeastern magnetic fabric that was observed in the Precambrian continental crust underlying the Niger Delta. I propose that the revised continent-ocean boundary (COB) occurs at the abrupt change between the northwest-trending Cretaceous magnetic anomalies and the Precambrian, northeast-trending crustal fabric. My gravity data modeling supports this revised location of the COB in the western and eastern Niger Delta.

I propose that these rifts are similar to Cretaceous rifts hosting large hydrocarbon discoveries to the west in Tano Basin (Ghana), the Cote d'Ivoire margin, and to the east in Equatorial Guinea and may contain similar syn-rift source with reservoirs also within the syn-rift section. The reservoirs are sealed by the base of the prograding Akata shales of the Niger Delta. Other potential source rocks may include the Cenomanian-Turonian interval in the overlying passive margin section.

Mayra D. L. Carrasquilla

Seismic Anisotropy of Granitic Rocks from a Fracture Stimulation Well at Utah FORGE Using Ultrasonic Measurements

For effective fracture stimulation in Enhanced Geothermal Systems (EGS), characterization of subsurface rock elastic properties is essential. As seismic anisotropy significantly influences hydraulic fracturing, locating and characterizing microseismic events, and forecasting stress trajectories and fracturing, our research undertakes laboratory experiments to study seismic anisotropy parameters of core samples from the Utah FORGE EGS site. We evaluated two rock samples from Well 58-32, at two depths of 2074.16 m (6,805 feet) and 2268.01 m (7,441 feet), respectively. We analyze the mineralogy and classify the shallower rock as syenogranite and the deeper rock as orthogneiss and monzonite. We cut cylindrical plugs from these two core samples, imaged them by computed tomography (CT) X-ray imaging, and measured their seismic properties in our anisotropy measurement system using ultrasonic waves at 1 MHz and under varying confining pressures (5-50 MPa) in ambient temperature conditions. With the assumption of transversely isotropic (TI) medium, we obtained three P-wave velocities and two S-wave velocities to calculate the Thomsen anisotropy parameters. The measured seismic velocities of each rock sample increase with increasing effective pressures, a behavior likely caused by closure of microcracks identified in the CT images. We also find that the measured anisotropies are higher at lower effective pressures. The maximum measured anisotropies for P-waves and S-waves are ~23% and ~30%, respectively. Therefore, we expect in the field operation that anisotropy should increase with increasing pore pressure cause by injection. These insights are valuable in future EGS reservoir management and monitoring.

Abstracts

Oral Presentations - SR1 223

Asmara Lehrmann

Fingerprinting paleoenvironments offshore Thwaites Glacier with modern foraminifera

Benthic foraminiferal assemblages are useful tools for paleoenvironmental studies but rely on calibrating live populations to modern environmental conditions. Here, we investigate the relationship between living foraminifera communities, collected during the austral summer of 2019, and their environment in the poorly constrained and difficult to access Thwaites Glacier in the Amundsen Sea. The ability to draw clear connections between living foraminifera communities and their environment, however, is essential for investigating past environmental changes in the vicinity of Thwaites Glacier, because it will better constrain fossil foraminiferal assemblage data as a proxy for water masses and their relative influence on glacial stability through time. Specifically, benthic foraminifera have been the potential to be used to reconstruct variations of relatively warm Circumpolar Deep Water, which is melting the floating termini of glaciers along Antarctica's Pacific margin, leading to retreat and, consequently, global sea-level rise. Using statistical models, we find two foraminiferal populations, which we refer to as the Adercotryma glomerata population and the Lagenammina tubulata population. These foraminiferal populations are likely controlled by proximity to the ice margins, oceanographic conditions, and sea ice cover. Sea ice cover influences foraminifera populations, as the available sunlight controls phytoplankton production thus, food supply for the foraminifera. Here, we also find a possible pioneer assemblage on the newly available substrate of the recently retreated Thwaites Glacier Tongue pinning point.

Md Upal Shahriar

Crustal structure and tectonostratigraphy of the Andaman oblique-subduction margin and its control on hydrocarbon potential

The highly-oblique subduction plate boundary in the Nicobar-Andaman Islands in the area north of Sumatra lacks active subduction-related volcanoes. It consists of 1) an active trench basin marking the zone of contact with the Indian oceanic plate, 2) a narrow, forearc basin that includes the Andaman Islands, and 3) a pull-apart basin with an active oceanic spreading center in a back-arc setting. In this study, I integrate gravity and magnetic with seismic reflection and well data to reveal the crustal structure of the area and the structural and bathymetric controls on sedimentation. The Andaman pull-apart basin was initiated as a broad zone of east-west-striking, normal faults in the Early Miocene that led to mantle upwelling and formed a 20-120 km-long spreading ridge in the Andaman Sea spreading center. Although the pull-apart basin lies at a depth of 3000m km and forms a major sediment sink, the spreading ridge underlies a 12-km wide valley in the sediments that are actively extending. Seismic reflection shows the Moho of oceanic crust extending 60 km north and, in some places, 100 km south of the spreading ridge and major tilting of the flanks of the spreading ridge. The east Andaman basin and Mergui ridge mark the contact of the Pull apart basin to the continental crust of East Asia. In this several inverted rifts related to the Oligocene Bampo formation of the Sunda continental block may act as habitats for oil and gas.

Abstracts

Oral Presentations - SR1 223

Amna Afzal

Quantification and Primary Source Analysis of Per- and Polyfluoroalkyl Substances (PFAS) in Edwards Aquifer and Neches River--- Southern Texas

Per- and polyfluoroalkyl substances (PFAS) have received remarkable attention in recent years as emerging contaminants. They are a family of fluorinated organic compounds with an anthropogenic origin. PFAS poses a risk to the human population and ecology due to their widespread usage in industry and their tendency to bioaccumulation. It is crucial to quantify PFAS in aquifers as they may act as a potential source of these toxins to humans and the associated ecosystem. The present study focuses on the quantification of 23 species (C4 to C12) of PFAS from different locations in the Edwards Aquifer and Neches River, Beaumont City Southern Texas from May to June 2023. The analysis of PFAS is completed by using triple quadrupole liquid chromatography-mass spectrometry (LC/MS-MS). The higher concentration of PFAS is found in Edwards Aquifer averaging 72.86 ppt as compared to the Beaumont samples averaging 62.34 ppt. In both the localities, there is an increase in short-chain species having 53% of total concentration especially downgradient due to their high mobility. Continuous monitoring of the distribution and quantitative speciation of PFAS in water systems in this area, which is currently in progress, would shed light on identifying their potential sources and facilitate possible remediation in the future.

Arya Tilak

Distribution, Age, and Significance of Cretaceous-Paleogene Intertrappean Beds in the Deccan Volcanic Province, India

The Deccan Volcanic Province (DVP) is an extensive igneous region, covering approximately 500,000 sq. km in NW Peninsular India. Erupted due to the Indian Plate overriding the Reunion hotspot (64-65 Ma), the DVP exemplifies a Continental Flood Basalt (CFBs). Notably, this volcanic province is associated with the Cretaceous-Paleogene (K/Pg) mass extinction event, which led to the extinction of the dinosaurs and several other life forms.

This study focuses on the intertrappean beds, sedimentary horizons of diverse origins, sandwiched between episodes of Deccan Basalt eruptions. Each intertrappean bed marks a period of 'quiescence' where life forms proliferated, offering essential clues about the extinction patterns and paleoenvironment during this critical geological period. The distribution and fossil content of these intertrappean beds are of paramount importance in comprehending Late Cretaceous life.

Furthermore, our research addresses the survival patterns of biota through the K/Pg transition, as well as the deposition and distribution of intertrappean beds. We also explore future research opportunities in this region. A crucial aspect of our study is to establish a consensus on the most representative section bearing the K/Pg boundary in India, as this remains a subject of debate due to the exclusive fossil evidence found in different sections. By examining the fossil content, flora, fauna, and climatic changes in each section, we aim to define the most suitable section for the Cretaceous-Paleogene Boundary in India. Through this comprehensive review, we shed light on the biota that prevailed during this significant time in geological history.

Abstracts

Oral Presentations - SR1 634

Karissa Vermillon

Resurrecting Rodinia: Who was our western neighbor?

Supercontinents are a natural part of the tectonic cycle, with the most recent and well-known being Pangea (~252 Ma). Before Pangea, there was Rodinia, which rifted around 750 Ma. Much less is known about Rodinia, especially regarding the question of the neighboring continent off the western margin of Laurentia. There are four models of Rodinia assembly relevant to the western Laurentian margin: (1) SWEAT – southwest Laurentia and eastern Antarctica, (2) AUSWUS – western US and south Australia, (3) Missing Link – South China block between western Laurentia and eastern Australia, and (4) Siberia Connection – Siberian shield and western Laurentia. Despite the concept of Rodinia being nearly 35 years old, there is still no consensus on which model is best. Many of these geologic based models hinge on correlations with southwest Laurentia, in which the San Gabriel Mountains (SGM) represent the furthest western margin. The most likely models are SWEAT or AUSWUS. There is a mismatch between the detrital zircon record between western Laurentia and the South China block (Missing Link) and most paleomagnetism studies rule out the Siberia Connection. Between SWEAT and AUSWUS, The SWEAT model is most appropriate, given the robust geologic match in 1.0-2.0 Ga basement rocks with the SGM. If southwestern Laurentia is a true tie-point, then the geochemical fingerprint of SGM basement and Neoproterozoic detritus should match with eastern Antarctica. A preliminary compilation of whole rock isotopic geochemistry and zircon Hf geochemistry between western Laurentia, south Australia, and eastern Antarctica shows striking similarities between all three and demonstrates the need for more data from Laurentia.

Divine Kalu

Mapping the Unknown: A Tale of Mineral Exploration, Inversion and Marvel of Invertible Neural Networks

As global demand for clean energy continues to escalate, ensuring a responsible and sustainable supply of critical minerals becomes paramount. This raises the need to improve and enhance the efficiency and accuracy of the processes and techniques involved in mineral exploration. The magnetotelluric (MT) technique which utilizes simultaneous measurements of the Earth's natural magnetic and electric fields as an electromagnetic induction source to map out the electrical conductivity variations in the Earth has been one of the very useful and widely applied method in mineral, geothermal, hydrocarbon and groundwater exploration. However, just like other geophysical methods, MT inversion suffers from severe non-uniqueness. Since the usefulness of an inverse solution hinges on understanding its uncertainty, it becomes important to quantify the uncertainties associated with each solution. We propose employing Invertible Neural Network (INN) as an alternative method for efficient estimation of resistivity structures and associated uncertainties. The INN establishes bijective mappings between resistivity models and MT measurements, incorporating a latent variable to capture the information loss during the forward process. Unlike conventional Bayesian inversion methods relying on computationally intensive Markov Chain Monte Carlo (McMC) sampling, INN offers fast inversion and uncertainty estimates with reduced computational overhead. To quantify model uncertainty, we simply drew 1000 samples from the posterior distribution by inputting the MT response and 1000 realization of normal Gaussian noise into INN and running it backward. We created 110,000 synthetic 1D resistivity models paired with MT responses, reserving 100,000 for training and 10,000 for testing. Numerical results based on synthetic data demonstrate INN's efficiency to adequately approximate the posterior distribution for the resistivity models with enhanced computational efficiency. We further applied this approach to a set of field data from East Tenant Region in Australia. Results from INN are highly consistent with previous studies and drilled wirelog data. Our work highlights the great potential of INN for solving the general electromagnetic inverse problem and quantifying its uncertainty.

Abstracts

Oral Presentations - SR1 634

Joe McNease

Surface wave workflows for the Texas Gulf Coast

The seismicity and crustal structure of the Texas Gulf Coast (TGC) is valuable information for future seismic monitoring related to carbon sequestration. We previously proposed to place 320 IGU-16HR nodes across 240 miles of the TX-LA Gulf Coast to monitor seismic activity related to ocean/lake noise and possible fault activity. To test the process of node deployment, retrieval, and data processing, we deployed 16 nodes across a study area in La Marque, Tx, and recorded seismic signals for 30 days. The cross correlation of the recorded ambient seismic noise can used for characterization of the near surface shear wave velocity structure. Applying ambient noise processing to the retrieved data results in the recovery of Rayleigh and Love wave Green's functions. We develop a processing workflow and suite of codes to use for future data collected from the TGC monitoring project.

Fnu Anshika

Development of an Analytical Method to determine of Airborne Phthalates

Phthalates (PAEs) are semi-volatile organic compounds (SVOCs) which are used as plasticizers and are added to polyvinyl chloride (PVC) for softening effects. They have high boiling point, low melting point and low vapor pressure which makes them appropriate to be used as plasticizers. PAE are not chemically bound to polymer matrix and thus, they get released from the products all throughout their lifecycle. These substances can be present in particulate as well as gaseous phase in ambient air. These plasticizers are ubiquitous in indoor and outdoor environments. In this study, we aim to target PAEs such as dimethyl phthalate (DMP), diethyl phthalate (DEP), dibutyl phthalate (DnBP), benzyl butyl phthalate (BBP), DEHP, and di-n-octyl phthalate (DnOP). These specific PAEs have been chosen for the study depending on their abundance, role in atmospheric chemistry and impacts on human health. All these PAEs are generally found in residential, commercial, and industrial areas, which makes them ideal target compounds for our study. This study is allowing us to develop a methodology for identification and quantification of PAEs in air in a major US city. For the development of an experimental analysis procedure, we are using a two-dimensional gas chromatography (2DGC-MS) system. It comprises a Shimadzu single quadrupole GCMS-QP2020 NX gas chromatograph-mass spectrometer (GC-MS) including two columns coupled to a Zoex ZX2 modulator, which allows two-dimensional gas-chromatography (2DGC) for separation of complex target matrices.

Abstracts

Oral Presentations - SR1 634

Mahmoudreza Momeni

Development of a Python-based Data Assimilation Framework (PyDAF)

Uncertainties in the input variables of atmospheric models are propagated into their results and degrade the ability of their predictions, which are used to estimate health effects and the uncertainty have negative impact on health estimations. In order to reduce the uncertainties, models can be constrained with observations as the optimal combination of the observed and modeled information can be utilized. Data assimilation technique combines observations and models in a way that accounts for the uncertainties in each while simultaneously respecting certain constraints. Data assimilation is a potent tool for investigating atmospheric phenomena, yet there currently exists no comprehensive framework (package) either in the United States or globally that can accommodate various methods and models effectively because the development of each data assimilation method, such as EnKF, 3DVAR and 4DVAR, is inherently complex, requiring advanced mathematical and probabilistic expertise. To address this gap, our research has led to the creation of a Python-based data assimilation framework (pyDAF), which supports the most widely used data assimilation approaches and integrates seamlessly with three of the main prestigious atmospheric models.

Anvesha Subramanian

A Novel Nanocarbon Infused Gum Arabic Sensing Skin Optimized for On-Skin Electronics and Temporary E-Tattoos

On-skin electronics are an emerging class of electronics fabricated using patterned inorganic and organic materials or nanomaterials on flexible substrates. However, current materials for on-skin electronics suffer from high cost to performance ratio, costly fabrication methodology and expensive precursor materials. Our research modified a skin-friendly, non-toxic water-soluble gum arabic matrix with multilayer graphene (MLG) to induce low sheet resistance resulting in a novel multi-property paintable nanocarbon infused nanocomposite optimized for on-skin electronics and temporary e-tattoos. Multilayer graphene in variable quantities were sonicated into an inexpensive, durable and water-soluble gum arabic medium and optimized for optimal amount of multilayer graphene (MLG) variable loadings (10-50%) and times (30mins-120mins) to find the optimal conditions for low sheet resistance. Sheet resistance tests found a generally linear increase in performance with higher loadings and sonication times and so, high sonication times were generally found to have a positive impact on conductivity due to quality of dispersion. However, in instances of 90-minute sonication times, performance degrades due to the increase in band gap. The results of this nanocomposites research created a highly adhesive, water-soluble and inexpensive electrically conductive carbon-based ink optimized for on-skin electronics and temporary e-tattoos costing < $0.1 per gram and optimum multilayer graphene-in-gum-arabic-glycerol formulations demonstrating competitive sheet resistance of 33.75 Ω/sq.

Abstracts

Oral Presentations - SR1 634

Kenneth Shipper

Flexural, crustal, and basin modeling of the Jurassic volcanic-clastic transition along the Guyana-Suriname margin

Understanding the distribution and maturity of Jurassic-Aptian source rocks along the hydrocarbon-prolific Guyana-Suriname margin requires understanding of its plate tectonic history, crustal structure, crustal types and their radiogenic heat production, heat flow history, stratigraphic evolution, and variations in overburden thickness. This study integrates seismic reflection and potential fields data to create a 3D model for the across-strike, continent-oceanic transition (COT) from the Guyana craton to the oceanic crust and the along-strike transition between the hotspot-influenced volcanic-rifted margin of the Demerara Plateau in Suriname to the non-volcanic, rifted margin in Guyana.

To create this 3D model of the Guyana-Suriname margin, I performed a 3D gravity inversion of the Moho constrained by seismic reflection and refraction controls integrated with a lateral velocity-density sedimentary inversion to a 2D KPSTM seismic grid.

In the seaward-dip direction, the non-volcanic rifted margin of central and northern Guyana consists of: 1) the 40-28-km thick, continental crust of the Guiana craton; 2) a 169-275-km wide, highly-tapered, necked zone of thinned continental crust with two parallel rift zones (Commewijne, Guyana); 3) oceanic crust that ranges in thickness from 10-15 km; and 4) the outer limit of the Jurassic oceanic crust is marked by the Demerara fracture zone that juxtaposes Jurassic oceanic crust of the Guyana basin with Cretaceous oceanic crust of the Equatorial Atlantic.

In the seaward-dip direction, the volcanic-rifted margin of Guyana-Suriname consists of: 1) the 40-21-km thick continental crust of the Guiana craton; 2) the 22-km-wide Commewijne rift, 3) the 25-km-thick SDR section related to the Demerara hotspot that locally created a 289-km-wide volcanic margin in Suriname and whose uppermost section has been dated as late Jurassic (173 Ma); and 4) the outer limit of the Jurassic oceanic crust is marked by the Demerara fracture zone that juxtaposes late Jurassic SDRs of the Demerara Plateau with Cretaceous oceanic crust of the Equatorial Atlantic. In the margin-parallel strike direction, the volcanic-rifted margin of Suriname consists of: 1): the thinned continental crust and oceanic crust flexed to the southeast beneath the load of the Demerara hotspot; 2) SDR units are thicker to the southeast (25-6 km) and thin to the northwest.

This model revealed three distinct regions along the strike of the Guyana-Suriname margin: 1) SDRs thin to the NW from 25-6 km over a range of 163 km. 2) Beneath these SDRs, the lower oceanic and thinned-oceanic crust dips to the southeast as a flexural response to the loading of the syn-rift SDRs related to the late Jurassic Demerara hotspot.

Hydrocarbon implications from this study include: 1) Late Jurassic source may be present in rifts of northern and central Guyana; 2) my maturity modeling indicates that maturity Cenomaian-Turonian source rocks on oceanic crust is limited; 4) Our maturity modeling shows that the flexed area marking the transition between the non-volcanic and volcanic margins formed a prominent basin low and sediment pathway (Berbice canyon) that promoted maturity in this area due to increased overburden thickness; 5) my model is validated by the distribution of productive wells and their gas-oil ratios.

Abstracts

Poster Presentations - Energy & Earth Resources

Ruth Beltran

Aptian-Albian tectonic evolution of a hyperextended, continental rift system and its transition into oceanic crust in the ultra-deepwater Campos basin, Brazil

The Campos Basin along the southeastern Brazilian margin was created by the Early Cretaceous rifting of continental crust between South America and West Africa. Two margin-parallel rift systems occupy the tapered zone of thinned, continental crust that underlies the passive margin section of the Campos basin: 1) Internal (or Merluza) rift system underlies the slope in water depths of 80-1500 m and is buried beneath 1 km of evaporites and 4 km of terrigenous clastic rocks of the passive margin; and 2) External rift system underlies in the ultra-deepwater area directly adjacent to the continent-ocean boundary, in water depths of 2600-3200 m, and is buried beneath 2 km of salt layers and salt diapirs of the passive margin; 2 km of Barremian syn-rift deposits and early Aptian microbialites were deposited in a pre-salt, sag basin that overlies an 11-km-thick crust, which previous workers have interpreted as either oceanic, thickened oceanic crust, ultra-thin continental crust, or exhumed mantle. The purpose of this study is to understand the tectonostratigraphic evolution of a hyperextended rift system of the External rift and to establish the thicknesses and distribution of the Lago Feia Group (Barremian), which is the most important syn-rift source and reservoir rock for giant oil fields located in the Internal rift. First, I use gravity and magnetic modeling to characterize the highly thinned continental crust of the External rift. Second, I use 450 km2 of 3D seismic data to characterize the sedimentary and magmatic of both the Barremian to early Aptian age rifts and the overlying, pre-salt sag basin of late Aptian age. To better characterize the crustal structure of the External rift, I tested four possible combinations of crustal types adjacent to oceanic crust, including 1) thinned continental crust, 2) oceanic crust, 3) exhumed mantle, and 4) pre-oceanic volcanic province. Based on the best fit with our structural and stratigraphic interpretations from seismic reflection data and gravity data, our preferred interpretation of the crust beneath the External rift zone is a 10-km thick, highly stretched, and thinned continental crust that is continuous with a thickened, pre-oceanic volcanic crust that transitions into a 6-km-thick, oceanic crust of Albian age. To better understand the sedimentary and magmatic history of the External rift, I use 450 km2 of 3D seismic data to characterize the sedimentary and magmatic of the Barremian to early Aptian age rifts and their overlying, pre-salt sag basin of late Aptian age. I interpret a hyperextended domain with a thick sequence of syn-rift carbonate rocks towards the southeastern part of the study area with scattered volcanoes in the central and northeastern areas of the study area. The syn-rift sedimentary sections are capped by a late Barremian sag sequence with carbonate buildups on horst blocks and sedimentary depocenters with potential source rocks in rifted lows.

Daniel Maya

Using gravity modeling to constrain the crustal structure of the Early Cretaceous volcanic-rifted margin of Uruguay

Cretaceous volcanic-rifted margins of the South Atlantic margin in Uruguay consist of up to 6-8-km-thick, magmatic-sedimentary flows manifested as “seaward-dipping reflectors” (SDRs) on seismic reflection data that dip in the direction of the spreading ridge. Previous workers have proposed three hypotheses for the origin of SDRs: 1) SDRs erupt directly onto areas of the exhumed mantle during a late rift stage as supported by some seismic reflection images that show prograding SDRs downlapping onto the Moho surface; this interpretation would imply that the earlier rift stage is non-volcanic in nature and resulted in the extrusion of the mantle in a “cold” rift environment with lower heat flows; 2) SDRs have erupted onto a proto-oceanic crust ranging from 5 to 7 km in thickness indicating a primitive form of oceanic spreading preceded the SDRs and provided a substrate for their later eruption; 3) SDRs erupted onto exhumed, lower continental crust along the distal domains of volcanic passive margins as proposed by previous workers for the conjugate Namibian margin. In this presentation, I test these three hypotheses for the crustal structure of offshore Uruguay using a 298-km-long, deeply penetrating seismic reflection line that crosses the Punta del Este Basin. The best-fitting gravity model along this reflection line supports the third hypothesis with a crustal structure of exhumed continental crust, overlain by a 6-km-thick section of SDRs and a crustal thinning point (CTP) that marks the landward limit of oceanic crust. This hypothesis for exhumed continental crust is further supported by total-horizontal and vertical-gradient gravity maps and reduced-to-pole magnetic maps generated for this study.

Abstracts

Poster Presentations - Energy & Earth Resources

Tessa Heaton

A Multifaceted Geochemical Study on Hydrocarbons and Energy Transition Avenues of the Bonaparte Basin, NW Australia

The Northern Territory Bonaparte Gulf Basin covers an area of approximately 270,000 km2 and is located on the northwestern margin of the Australian shelf (Bonaparte Basin, 2023). Stratigraphy of the region provides excellent source, reservoir, and trap intervals from significant geological events of rifting, extension, and salt tectonics (Geoscience Australia, 2023). The Bonaparte Basin has been a well-known hydrocarbon play fairway since the early 1960s when high quality reservoirs were first unveiled (Sazali et al, 2021). Despite a heavy production region, the Bonaparte Basin has faced market limitations with remaining reserves estimated at 33.42 GL of oil and 668.55 BCM of gas (Geoscience Australia, 2023). This study serves as a hydrocarbon potential reassessment of ten wells as well as their potential for energy transition avenues, for instance enhanced oil recovery (EOR), carbon capture storage (CCS), and hydrogen production (H2). The core and cuttings data utilized for this project is published in a petroleum exploration report submitted to the Northern Territory Government (Australia) in 1984, under all applicable petroleum legislation. The data is publicly available at the Northern Territory Geological Survey Core Library online repository (Northern Territory Government, 1984) and contains Rock Eval data, vitrinite reflectance information, n-alkane compositional data, and the relative proportion of saturate, aromatic, resin (NSO), and asphaltene fractions. Rock eval pyrolysis data will be used to determine kerogen type, conduct thermal maturity assessments, correlation between wells, and lithofacies. Molecular chemistry will be used for assessments of organic sources and paleo-depositional environments of the basin rocks. Trends can be seen in kerogen type, molecular cross plots, and maturity data across all wells. Understanding organic richness, kerogen type, thermal maturity, correlations between wells, and lithofacies is essential to understanding petroleum systems. By combining molecular proxies with Rock Eval data, a more comprehensive characterization of these basin rocks will be achieved and will ultimately provide the data needed for an overall reassessment appraisal for the ten wells. This study is expected to improve assessments of geochemical signatures of a petroleum system and better define prospect areas with the potential to host hydrocarbon accumulations. As for the future of resources in Bonaparte, there are potential opportunities for EOR, CCS, and H2 generation.

Mohammad Jahirul Alam

Investigating the Complexities of VOC Sources in Mexico City in the Years 2016–2022

Volatile organic compounds (VOCs) are major ingredients of photochemical smog. It is essential to know the spatial and temporal variation of VOC emissions. In this study, we used the Positive Matrix Factorization (PMF) model for VOC source apportionment in Mexico City. We first analyzed a data set collected during the ozone season from March–May 2016. It includes 33 VOCs, nitrogen oxide (NO), nitrogen dioxide (NO2), the sum of nitrogen oxides (NOx), carbon monoxide (CO), sulfur dioxide (SO2) and particle matter with a diameter < 1 μm (PM1). Another PMF analysis focused only on VOC data obtained in the month of May between the years 2016, 2017, 2018, 2021, and 2022 to gain insights into interannual variations. While the use of fossil fuel through combustion
and evaporation continues to be major fraction in Mexico City, additional sources could be identified. Apart from biogenic sources which become more important closer to the end of the ozone season, a second natural emission factor termed “geogenic”, was identified. Overall, anthropogenic sources range between 80–90%. Diurnal plots and bivariate plots show the relative importance of these emission source factors on different temporal and spatial scales, which can be applied in emission control policies for Mexico City.

Abstracts

Poster Presentations - Energy & Earth Resources

Muhammad Younas

Geospatial analytics of driving mechanism of land subsidence in Gulf Coast of Texas, United States

Land subsidence has been an ongoing issue for over a century along the Gulf Coast of Texas in the United States. This study assesses and models the factors contributing to land subsidence covering fifty-six (56) counties along the Gulf of Mexico coastline from Louisiana to the border of Mexico, approximately 300,000 km2. Geospatial statistical techniques and regression models were employed to investigate and predict the fundamental causes of land subsidence by integrating multiple datasets such as Global Navigation Satellite System (GNSS) (147 stations), groundwater extraction (78,420 wells), hydrocarbon production (84,424 wells), precipitation, and population growth. In the last two decades, the overall population rose by 33 % and the compound annual population growth rate increased from 2.08 to 4.10 % in Montgomery, Waller, Fort Bend, and Chambers counties. Emerging hotspot analysis reveals that the groundwater level is persistently declining and the regression model (R^2= 0.92) tested over Harris County predicts that the population growth significantly contributes to land subsidence in this region. The groundwater withdrawal rate is increased from 23 to 96.6 billion gallons in Harris, Montgomery, and Fort Bend counties in the last two decades. A prolonged drought from 2010 to 2015 due to low precipitation affected all fifty-six counties. Oil production increased eightfold and a high extraction rate of 19.5 to 40.1 million bbl/yr of oil in Karnes County was recorded within the last 20 years. The regression model (R^2 = 0.73) over this county suggests that oil extraction is a primary contributing factor to the observed subsidence. Although the gas extraction rates for all counties are decreasing over time, some counties in the southern part of the Gulf Coast Aquifer show relatively higher extraction rates. For the first time, this research determines that all fifty-six counties along the Gulf Coast of Texas are undergoing land subsidence and experiencing high population growth, groundwater withdrawal, and hydrocarbon extraction.

Abstracts

Poster Presentations - Earth & Planetary Dynamics

Johanna Villagomez

Monitoring ground motions caused by possible shore fault movement and ocean waves

Offshore Texas in the Gulf of Mexico harbors numerous geological faults who potential seismic activity remains poorly understood. This research aims to investigate the presence of microseismic events associated with fault movements and oceanic disturbances. Using seismic nodes, we propose to monitor ground vibrations induced by seismic activities. The seismic nodes, designed as compact, waterproof units with minimal environmental impact, are strategically placed to capture ground vibrations. 320 nodes will be deployed within 30 miles of the coastline along the Gulf Coast from Corpus Christi to the TX-LA border, approximately 240 miles. The proposed deployment of seismic nodes will take place between December 2023 and August 31, 2024. The significance of this research lines in its potential to fill critical gaps in understanding offshore fault dynamics, ultimately contributing to scientific advancements and support both graduate and undergraduate research endeavors.

Presley Greer

Detecting subsurface ice wedges using GPR at the CRREL Permafrost Tunnel in Fox, Alaska

The warming of Alaska's permafrost has been leading to thawing within its discontinuous permafrost. This can cause ice wedges to melt resulting in thermokarst formations such as sink holes and landslides which are causing damage to Alaskan infrastructure. To avoid developing further infrastructure in areas containing ice wedges, it is necessary to improve methods of detecting subsurface ground ice. Ground Penetrating Radar (GPR) is a nonintrusive remote sensing method of locating and characterizing permafrost and other subsurface features that are not evident on a cut face or surface. When applied to the detection of ice wedges at the CRREL (Cold Regions Research and Engineering Laboratory) permafrost tunnel in Fox, Alaska, a few identifying features were observed which corresponded with prior research. We first used GPR reflections of areas along the tunnel walls holding known ice wedges to verify the identifying features of an ice wedge within GPR data. We utilized these reflections as test data to identify possible ice wedges in locations where they were not observed on the tunnel walls.

Mikaela Garcia

Quantifying Erosion at Sargent Beach, Texas Using Remote Sensing

Hurricane Nicholas, a category 1 hurricane, hit Texas on September 14, 2021, making landfall 10 miles west of Sargent Beach. The hurricane caused an estimated loss of $1.1 to $2.2 billion. With wind gusts up to 95 mph, the hurricane knocked down trees and heavy rains caused 20 inches of standing water. The shoreline of Sargent Beach is one of the most rapidly eroding shorelines along the Texas coast, in part due to storms such as Hurricane Nicholas, which caused heavy erosion and accelerated the rate erosion. In this area, major storm events remove sediments that would normally be replaced by the Brazos River, but the river and its drainage basin have been altered so that the sediments no longer reach Sargent Beach. For this reason, morphological changes occur rapidly in this area at the expense of the shoreline and dunes on this beach. This study used high-resolution digital elevation model (DEM) acquired by Unmanned Aerial Vehicle (UAV) and LiDAR acquired in 2018 to assess the damages and recovery of the beach. UAV-based lidar data was acquired in May 2023 and December 2023. We have created digital elevation models, digital surface models, and orthomosaics. In addition, several Landsat images before and after the Hurricane, as well as aerial photographs, were used to quantify the changes. These datasets were processed to determine the rate of erosion of the coastline and the changes that occurred to the coastal dunes during this time frame.

Abstracts

Poster Presentations - Earth & Planetary Dynamics

Joshua Miller

Paleogene arc collision and migration in the Bering Sea interpreted from regional magnetic and gravity data

Previous workers agree that most of the Aleutian arc began in the Middle Eocene (~50 Ma) following a large, 500-km, southward step from its former position along the northeastern Bering Sea margin along Alaska and the Russian Far East. These earlier tectonic interpretations were carried out during the 1970s and 1980s and were based mainly on outcrop studies and widely-spaced wells. In addition, regional gravity and magnetic data were more fragmented and not as accessible and continuous as they are today. In this presentation, I extract data for the Bering Sea area from global gravity and magnetic data sets to illustrate the continuity of several major tectonic features along both the Alaskan and Russian continental margins that include: 1) These maps highlighted the high responses of gravity and magnetics characteristics which constrained the oceanic crust; 2) the proto-Aleutian, intra-oceanic arc that accreted to the Bering Sea margins during the Paleocene-early Eocene; the arc is relatively narrow, forms a bathymetic dome, exhibits a continuous, magnetic and gravity high, and is bounded on its seaward side by a thrust and filled trench and on its landward side by a linear, right-lateral strike-slip fault; 3) the area of continental Alaska and the Russian Far East has been previously described as a Cretaceous and older arc terrane and exhibits a distincitve magnetic signature that differs from the adjacent, elongate arc; 4) the interior of the Bering Sea exhibits no organized oceanic spreading fabric or linear hotspot tracks; its crustal thickness of ~15 km indicates an oceanic plateau origin; and 5) the wishbone-shaped junction of the proto-Aleutian arc along the Bering Sea with the modern Aleutian arc is the area where the two arcs separated in Late Eocene time. The proposed tectonic history of the area includes the insertion of the proto-Aleutian arc into the region, its Paleogene collision with the margin of Alaska and the Russian Far East, the termination of subduction along the northern Bering Sea margin with the southward jump in subduction to the modern Aleutian arc - which acted to capture the large oceanic plateau in the Bering Sea. I also compile tomographic data from previous workers to show the location of the subducted Pacific slab beneath the Bering Sea whose length supports its initial subduction age of 50 Ma.

Jennifer Welch

Unveiling the Hidden Threat: Drought-Induced Inelastic Subsidence in Expansive Soils

Expansive soils pose a significant challenge in geotechnical engineering, especially in coastal areas. While research has mainly focused on their elastic properties, this study explores the overlooked aspect of inelastic subsidence during prolonged droughts, utilizing decade-long GPS datasets from the University of Houston Coastal Center. Our findings reveal substantial subsidence, approximately one to two dm, during the summer droughts of 2018, 2020, 2022, and 2023, due to compaction within the upper 4 m of expansive soils. Inelastic subsidence constitutes roughly 10% of the total subsidence, resulting in step-like permanent land elevation loss over time. Notably, drought-induced subsidence is prominent in open-field areas with expansive soils but is minor in built-up areas or in non-expansive soil regions. The occurrence of inelastic subsidence challenges traditional assessments of relative sea-level rise and coastal flooding, emphasizing the need to consider it in coastal infrastructure planning for enhanced resilience against climate uncertainties.

Abstracts

Poster Presentations - Earth & Planetary Dynamics

Muhammad Asif

Improving InSAR Measurements: The Role of High-Resolution LIDAR DEMs in Topographic Correction

High resolution DEMs are crucial for InSAR, enhancing accuracy in topographic adjustments. This study evaluates the accuracy of eight different Digital Elevation Models (DEMs) by comparing them with high-resolution LiDAR data over portions of the state of Florida. The DEMs assessed include SRTM 30, Copernicus DEM, ASTER GDEM, ALOS, TanDEM-X 90, X-SAR DEM, Merit DEM, and NASA DEM. Each DEM was processed using standard geospatial techniques, such as mosaicking, reprojection, resampling, and cropping, to fit the study area in a consistent projected coordinate system of NAD83(2011) / Florida GDL Albers with a resolution of 90 meters. Visualization techniques such as; hill shading, slope, and aspect maps were employed to illustrate the terrain representations provided by each DEM. Statistical measures, including mean, standard deviation, average slope, and average aspect, were computed to quantify and compare the properties and quality of the elevation data among the DEMs. The key aspect of the research involved creating error rasters through the raster calculator tool in QGIS, which entailed subtracting LiDAR-derived elevation data from each DEM on a cell-by-cell basis. This method allowed for a precise comparison and highlighted discrepancies between the DEMs and the high-resolution LiDAR data. The results are visually presented using box plots, which detailed the variance and distribution of errors across the datasets. Moreover, the high-resolution and accuracy of the LiDAR DEM are critical in applications such as Interferometric Synthetic Aperture Radar (InSAR) that require precise elevation information to measure earth deformation, analyze land subsidence, and monitor environmental changes effectively. Using high-resolution DEMs like LiDAR instead of SRTM can significantly enhance the accuracy in reducing the topographic effects from InSAR results, assist in georeferencing, contribute to interferogram generation, support phase unwrapping, and aid in baseline calculations, thereby providing more reliable data for geospatial and environmental analysis. These functionalities ensure accurate surface deformation measurements and enhance the reliability of geospatial data integration, making high-resolution DEMs like LiDAR invaluable for advanced geospatial analyses. This comprehensive assessment provides valuable insights into the relative accuracies of globally available DEMs when benchmarked against precise LiDAR data, emphasizing the importance of careful selection and processing of elevation data for regional studies in geospatial sciences.

Kaitlyn Bryant

Using a compilation of vintage seismic reflection data and earthquake data to understand the tectonic origin of the Puerto Rico-Virgin Islands Arch

Puerto Rico is known for its rich geologic history, and for as long as it's been studied, it has been known to have formed a large anticline with average dips of 4 degrees on the northern, more gentle limb of the fold and steeper dips of up to 30 degrees on the steeper-dipping southern limb due to the motion of the North American Plate and the Caribbean plate. This formation is called the Puerto Rico-Virgin Islands Arch. There is ample evidence of the motion of the two plates forming this anticline, but the nature of their movement is not as obvious to understand. Because motion between the two plates is highly oblique, the region exhibits characteristics of both subduction and strike-slip faulting. To the north of the island, the Puerto Rico trench marks the location where the North American Plate obliquely subducts to the south beneath Puerto Rico, and to the south of the island, the Muertos trench marks the location where the Caribbean Plate obliquely subducts to the north beneath Puerto Rico. This presentation aims to better understand how this complex tectonic setting has formed a major structural and topographic feature exposed onland and offshore in Puerto Rico and the Virgin Islands called the Puerto Rico-Virgin Islands Arch. Two hypotheses for the arch include: 1) the arch formed as the result of tectonic erosion of the northern and southern forearc areas of Puerto Rico which acted to drop the two fold limbs downward in a non-compressive manner; and 2) the arch formed as the result of convergence of the two subduction zones with the possibility of the two slabs colliding at depth beneath the island. This study will utilize three vintage seismic datasets, but provided by primarily Western Geophysical Company that dates back to 1974. With this data, I have made a structure map on the top of the island arc basement of the island along with the key Oligocene to Pliocene sedimentary units that overlie the basement. These data show that the age of the arch is Pliocene and younger. I have also compiled earthquake data from the Puerto Rico Seismic Network to show how the shallower-dipping southern slab creates more deformation in the arch relative to the steeper dip of the northern slab. As I saw no evidence of subduction erosion in the forearc areas, I conclude that Pliocene and younger convergence between the two subduction zones are the mechanism for the formation of the arch.

Abstracts

Poster Presentations - Atmospheric & Earth Surface Systems

Samantha Baker

Temporary Sediment Storage in Proglacial Lakes Near Kangerlussuaq, Greenland

Proglacial lakes along the western margin of the Greenland Ice Sheet serve as temporary reservoirs for freshly weathered sediment, which is subsequently transported downstream by braided rivers and is deposited in adjacent fjords. These lakes have the potential to generate glacial outburst floods, known as jökulhlaups, when the ice or moraine that dams them becomes destabilized. The town of Kangerlussuaq, located in Southwest Greenland, has a history of jökulhlaups. In 1987, Kangerlussuaq experienced a jökulhlaup of 32–36 × 106 m3 water discharge in 36 hours (Russell 1987). Following this event, there was a period of dormancy, with no jökulhlaup until 2007 when the town witnessed its largest recorded jökulhlaup, discharging up to 39 ± 10.8 x 106 m3 of water over a 17-hour period. Since 2007 the area has experienced jokuhlhlaups nearly every year, with notable events in 2008, 2010, 2011, 2012, 2014, and 2015 (Carrivick et al. 2017). These catastrophic events entrain sediment from the proglacial lakebed, resulting in downstream sediment-laden flows exceeding 3,000 mg/L. The objective of our study is to estimate sediment delivery and deposition for seven proglacial lakes near the Russel Glacier margin in Kangerlussuaq. During the Summer of 2023, we measured suspended sediment concentration (SSC) of the water surface at lake inlets and outlets and obtained bathymetric data of the lake bottom. We apply the Normalized Difference Suspended Sediment Index (NDSSI) to Sentinel-2 satellite data to determine a correlation between measured and predicted SSC. We then extract streaklines to monitor changes in SSC and identify areas experiencing net deposition and erosion of sediment. By examining the relationships between sediment delivery and proglacial lake morphology, we aim to estimate local sediment transport and storage. The outcomes of this study will contribute valuable insights into sediment transport to the coastal regions of Greenland and enhance our ability to predict natural hazards related to jökulhlaup.

Sagar Rawak

Use of GPS to study the Land Subsidence and it's effects in Harris County

The Harris country has suffered a potential land subsidence due to excessive pumping of groundwater and natural oil and gas in past several years. The continuous subsidence is threat to people life and economy as it is major contributing factors for flooding, infrastructure damage, ruptures of land surface and reduce the capacity of aquifers that can results in huge economic loss. The Gulf Coast aquifer system in the Houston area is uniquely susceptible to clay-compaction and subsidence due to its aquifer composition and large amounts of historical groundwater withdrawal. The primary cause of land subsidence is due to presence of unconsolidated sediment deposits. When water table is lowered, it triggers the land subsidence. Harris county is primary composed of three aquifer chicot, Evangeline and Jasper. The Houston region has been suffering from subsidence caused by excessive groundwater withdrawals in lates 2000s which has been reduced significantly by use of more surface water then groundwater. This study compromises the study of GPS data ,aquifer well data, natural gas and well data from North West to South East Region to measure the subsidence rate. It has been found that the north west regions still suffers high subsidence rate due to large population and presence of active natural and gas wells. This study suggests that the Evangeline aquifer is found to be the primary cause of subsidence.

Abstracts

Poster Presentations - Atmospheric & Earth Surface Systems

M. Ahmad

Machine learning models for an Ozone Episode in Mexico City

Mexico City, located in the tropics within a basin with an altitude ~2240 meters above mean sea level and surrounded by mountains on three sides with an opening to the north, experiences ozone episodes due to its specific topography and strong ozone precursors emissions. This necessitates constructing a model that can rank meteorological and air pollution variables according to their contributions to the build-up of ozone during an ozone episode in Mexico City. Such ranking is important for regulatory procedures targeting at reducing ozone harmful effects during an ozone episode on a local scale. In this study, machine learning models including Random Forest, Gradient Boosting Tree, and deep neural network are utilized to learn functional dependence of ozone on the selected meteorological and air pollution variables and predict hourly ozone concentrations using hourly data of eight predictors (nitric oxide, nitrogen dioxide, shortwave ultraviolet-A radiation, wind direction, wind speed, relative humidity, ambient surface temperature, planetary boundary layer heigh). And the deep neural network with 92% accuracy together with Shapely Additive exPlanations approach is used to simulate high ozone concentrations and rank the predictors according to their importance in the build-up of ozone during 6 to 18 March 2016, this period includes an ozone episode. The proposed research can be utilized to any other City in the world.

Kennedy Potter

Subaqueous Carbon Sequestration in Elephant Butte Reservoir, New Mexico

The American West is a semi-arid region that experiences seasonal monsoon-driven flooding and is home to many inland reservoirs. While covering less than 2% of the Earth's surface, inland waters bury an estimated 0.15 Pg C/year compared to oceans which bury 0.20 Pg C/year, with reservoirs burying 40% of the organic carbon (OC). The Elephant Butte Reservoir (EBR) along the Rio Grande in New Mexico is characteristic of these conditions. It is fed primarily by summer monsoons (July-October) and spring snowmelts (April-June), which bring sediment into the reservoir and sequester OC through delta building and hyperpycnal plumes. This research aims to quantify subaqueous carbon storage at EBR, providing insight into the importance of inland reservoirs as carbon sinks. On the first weekend of March 2024, the authors conducted a boat-based field campaign using locations informed by bathymetric data collected by the U.S. Bureau of Reclamation in 2019 as well as wetted frequency maps generated from applying the Normalized Difference Water Index to Landsat 8 and 9 images. At each location, the team collected conductivity, temperature, and depth data using a SonTek CastAway CTD, water samples using a Van Dorn-style sampler, and sediment samples using a Petite Ponar grab sampler. The samples were then transported to the Sedimentology Lab at the University of Houston Department of Earth and Atmospheric Science where the sediments were analyzed for grain size distribution using a CILAS 1190. Suspended sediment concentration was found using a vacuum to pull the water samples through a filter then measuring the weight of the sediment caught. Loss on ignition will be used to assess the organic matter content of the sediment samples. Current findings indicate grain sizes ranging from 4.68 μm to ~6 cm and suspended sediment concentrations ranging from 4 to 12 mg/L. This study is expected to yield results that show that higher concentrations of organic carbon are focused in areas that are more often inundated (i.e., less frequently exposed to air) and lower concentrations are focused in areas that are inundated less often. Ultimately, this study will inform the spatial distribution of carbon sequestration at EBR which holds important implications for dams across the Western United States.

Abstracts

Poster Presentations - Atmospheric & Earth Surface Systems

Caroline Mandujano

Investigating Downstream Fining in Kangerlussuaq, Greenland

In channelized flow, sediment fines downstream as a result of hydrodynamic sorting, abrasion and attrition, and chemical weathering processes. While high latitudes typically experience limited chemical weathering, this does not hold true for glacierized catchments. Alpine glaciers, for example, exhibit chemical weathering rates comparable to or even exceeding the global average. Given the substantial yield of freshly weathered sediment from retreating glaciers, and as a result of this sediment being physically abraded and strained, it readily reacts with meltwater through dissolution. Thus, meltwater flux is the primary control on chemical weathering in glaciers. A global rise in meltwater discharge from glaciers, driven by increased atmospheric temperatures, could potentially impact chemical weathering rates and the grain size of sediment exported from glaciers. This research intends to explore the mechanisms and impacts of downstream fining in a glacierized catchment located in Southwest Greenland. Specifically, we seek to test the following hypothesis: In this catchment, downstream fining cannot be solely attributed to hydrodynamic sorting and physical weathering mechanisms; chemical weathering is necessary to explain the observed fining trends from source-to-sink. Our study site, Kangerlussuaq, hosts a braided river system that emerges from three land-terminating lobes of the Greenland Ice Sheet. At the ice margin, referred to as the sediment 'source,' we observed terminal moraines comprised of poorly sorted, coarse and fine sediment. The sediment 'sink' is defined as the marine fjord waters, where the braided system constructs a delta and an extensive, sinuous turbidity current channel. Within a distance of approximately 31 kilometers, the sediment composition undergoes a size transition, shifting to predominantly well-sorted, medium- to fine-grained sand in the submarine channel with clays to silty clays on its flanks. To test our hypothesis, sediment samples were collected for grain size and mineralogical analyses. Water samples were collected for cation and anion analysis, enabling us to derive ion denudation rates as a proxy for chemical weathering rates. We expect to find that chemical weathering produces discrepancies in downstream fining rates based on mineralogy.

Leo Collier

Monitoring Seaward Dune Recovery on Matagorda Peninsula

The Texas Gulf Coast Barrier Islands have a dynamic and delicate dune system that sees seasonal change influenced by various natural and anthropogenic factors. This work is part of ongoing research that seeks to monitor and record changes in sedimentation, erosion, and overall dune stability to better understand and protect this delicate system. In this study, we examine the 5-year period between Hurricane Harvey and the most recent field survey on Matagorda Peninsula in the central Texas coast. Using drone-based LiDAR, photogrammetry, and historical LiDAR data we can observe and quantify changes and track the seaward recovery of a hurricane damaged dune system on the Matagorda Peninsula. Our findings highlight the resilience of these coastal systems and provide valuable insights for coastal management and conservation efforts.

Abstracts

Poster Presentations - Atmospheric & Earth Surface Systems

Alejandro Aguilar

Unraveling the Subsurface Story: Investigating Fluvial Sedimentology of the Rio Grande Using Ground Penetrating Radar

Ground Penetrating Radar (GPR) has been proven effective in numerous case studies, particularly when the primary objective is to employ a non-intrusive method of surveying to investigate subsurface anomalies. Elephant Butte State Park, situated 5 miles from Truth or Consequences, New Mexico, hosts the largest reservoir in the state: Elephant Butte Lake. Constructed in 1915, this reservoir is crucial to the Rio Grande Project, which aims to provide power and irrigation to south-central New Mexico, western Texas, and northern Mexico. The Rio Grande, coursing through the reservoir, oversees the sediment deposition flowing towards the lake and to the Gulf of Mexico. The study area, which remains wet almost 70 percent of the year and lies north of Elephant Butte Lake, is encircled by an active depositional bank. During flood events, water flows through this area and drains into the Rio Grande via a channel known as a Tie Channel. Utilizing the 250 MHz Noggin GPR system, six lines-three perpendicular and three parallel to the river-were conducted to comprehend the fluvial sedimentology of the river. Each line underwent analysis using EKKO sensors and software, revealing features such as channel infill, incisions (concave-up bounding surfaces), bars (convex-up surfaces), and levee deposition. The objective for the survey is to reconstruct past depositional environments and reveal the nature of sedimentary processes, thereby assisting in hydrocarbon reservoir studies.

Irfan Karim

Investigating the anthropogenic sources: Methane and Carbon Dioxide Emissions in Houston, Texas

Identifying carbon dioxide (CO_2) and methane (CH_4) emissions in Houston is crucial for understanding their impacts from various sources. These gases can originate from both natural and human-related processes. Carbon isotope ratios, specifically $\delta^{13}CCH_4$ and $\delta^{13}CCO_2$, are effective tools for source differentiation.

Using a cavity ring-down spectrometer, we conducted measurements of CH_4, $\delta^{13}CCH_4$, CO_2, and $\delta^{13}CCO_2$ at the Moody Tower throughout 2022. The data revealed that CH_4 concentrations peaked at 2.4 ppm when winds blew from the N-NE to SW, while CO_2 levels rose to 440 ppm when winds came from the NE-NW. $\delta^{13}CCO_2$ values were more negative (-17‰) with northern winds and lower $\delta^{13}CCH_4$ (-50‰) when winds originated from the south and southeast.

Canister measurements were used to determine $\delta^{13}CCH_4$ and $\delta^{13}CCO_2$ signatures from specific emission sources like wetlands and car exhaust. Downwind from car exhaust, CO_2 and CH_4 emissions were elevated, with concentrations of 16887 ppm and 15 ppm compared to 426 ppm and 1.92 ppm upwind. $\delta^{13}CCO_2$ shifted significantly to -24‰ downwind compared to -12‰ upwind similarly $\delta^{13}CCH_4$ also shifted to -21 from -47‰ upwind. In McCarty landfill samples, downwind CO_2 increased marginally to 422 ppm from upwind values of 413 ppm. CH_4 values also increased significantly, with 2.02 ppm upwind and 5.92 ppm downwind, along with identical mean isotopic ratios of -14‰ for $\delta^{13}CCO_2$ and -56‰ for $\delta^{13}CCH_4$ in both directions.

These results highlight those daily variations in CH_4, $\delta^{13}CCH_4$, CO_2, and $\delta^{13}CCO_2$ concentrations result from diurnal changes in emission intensity and atmospheric processes.

Abstracts

Poster Presentations - Atmospheric & Earth Surface Systems

Jincheol Park

First Top-Down Diurnal Updates to NOx Emissions Inventory in Asia Informed by the Geostationary Environment Monitoring Spectrometer (GEMS) Tropospheric NO2 Columns

Pioneering the use of the Geostationary Environment Monitoring Spectrometer's (GEMS) observation data in air quality modeling, we updated Asia's NOx emissions inventory by leveraging its unprecedented sampling frequency. GEMS tropospheric NO2 columns served as top-down constraints, guiding our Bayesian inversion to hourly update NOx emissions in Asia during spring 2022. This effectively remedied the prior underrepresentation of daytime NOx emissions, significantly improving simulation accuracy. The GEMS-informed update reduced the extent of model underestimation of surface NO2 concentrations from 19.23% to 11.36% in Korea and from 12.85% to 4.42% in China, showing about 6% greater improvement compared to the update based on the sun-synchronous low earth orbit observation proxy. Improvements were more pronounced when larger amounts of observation data were available each hour. Our findings highlight the utility of geostationary observation data in fine-tuning the emissions inventory with fewer temporal constraints, thereby more effectively improving the accuracy of air quality simulations.

Xinyue Wang

Global Energy Imbalance of Saturn

The global energy budget is pivotal to understanding planetary evolution and climate behaviors. Assessing the energy budget of giant planets, particularly those with large seasonal cycles, however, remains a challenge without long-term observations. Evolution models of Saturn cannot explain its estimated Bond albedo and internal heat flux, mainly because previous estimates were based on limited observations. Here, we analyze the long-term observations recorded by the Cassini spacecraft and find notably higher Bond albedo (0.41 ± 0.02) and internal heat flux (2.84±0.20 Wm-2) values than previous estimates. Furthermore, Saturn's global energy budget is not in a steady state and exhibits significant dynamical imbalances. The global radiant energy deficit at the top of the atmosphere, indicative of the planetary cooling of Saturn, reveals remarkable seasonal fluctuations with a magnitude of 16.0±4.2%. Further analysis of the energy budget of the upper atmosphere including the internal heat suggests seasonal energy imbalances at both global and hemispheric scales, contributing to the development of giant convective storms on Saturn. Similar seasonal variabilities of planetary cooling and energy imbalance exist in other giant planets within and beyond the Solar System, a prospect currently overlooked in existing evolutional and atmospheric models.

Abstracts

Poster Presentations - Atmospheric & Earth Surface Systems

Thishan D Karandana

Impact of California Wildfires on Atmospheric Trace Gases

This study leverages satellite data and chemistry transport models to analyze the impact of wildfires on trace gases in California during the August-October periods of 2018, 2019, and 2020. During these months, Southern California experiences minimal precipitation, leading to high Vapor Pressure Deficit (VPD), which in turn results in decreased photosynthetic activities. This reduction, combined with the increase in biomass burning, causes a rise in CO2 concentrations, as observed by the OCO-2 satellite. The dry season also witnesses increased CO and CH4 levels, tied to the surge in biomass burning, as detected in TROPOMI retrievals. The CarbonTracker model captures these elevated CO2 concentrations, though with a somewhat reduced amplitude. Similarly, the GEOSChem model successfully simulates higher CO levels but underestimates the observed enhancements. These findings will contribute to an improved understanding of fire's influence on trace gases and aid in refining future numerical models.

Daniel Ragusa

Tracking the water pH and atmospheric CO2 evolution during synthetic carbonate precipitation

Paleo-CO2 reconstructions are valuable in understanding the fluctuating of Earth's past climate and assessing its reaction to such changes by learning the present. The present is the key to demystifying the past, and the past is critical to predict the likely changes in the future, among these are the Earth's response to potential increases in anthropogenic CO2. Past CO2 reconstructions are possible using stable isotope proxies. However, field and archive specific measurements that develop such proxies do not have laboratory calibrated results to serve as a metric for their reconstructions. In this research, laboratory experiments will be performed. Both biogenic and abiogenic calcium carbonate will be precipitated in a laboratory constrained environment, with known temperature and pressure in an enclosed atmosphere. These synthetic carbonates will archive the changes performed inside that environment, and we will monitor the changes in the water's pH and CO2 evolution inside that atmosphere to assess the rate of CO2 sequestration during synthetic carbonate precipitation. We will use the Aerodyne Tunable Infrared Laser Direct Absorption Spectroscopy (TILDAS) of the PaleoGeochem research group to monitor the CO2 evolution of this synthetic atmosphere and to measure its corresponding stable isotopic signatures. Doing this experiment will allow us to track the evolution of CO2 during the precipitation process as well as monitor how pH of the solution changes during the process. We hypothesize that the stable oxygen isotope signatures for biogenic and abiogenic carbonates in water are different. We expect that these carbonates and information from this constrained environment monitoring will serve as a reference for field-collected samples for modern environment calibration and for future research on paleoclimate reconstruction. This research can additionally bring new insights into the tracking of CO2 injected plumes from carbon capture utilization and storage (CCUS) technologies using stable oxygen isotopes.

Abstracts

Poster Presentations - Atmospheric & Earth Surface Systems

Nilay Gungor

Proglacial Delta-Front Sediment Transport in West Greenland

Arctic coastal zones are experiencing rapid change due to the melting of glaciers and permafrost driven by an increase in atmospheric temperature. As a result, sediment delivery to the Southwest coast of Greenland is rapidly building fjord deltas. The aim of our research is to understand the partitioning of sediment between the subaerial and subaqueous delta for these systems by quantifying delta-front sediment transport. To address this, we conducted surveys of the Quinnguata Kuussua river delta front in Kangerlussuaq, Greenland in Summers 2022 & 2023. We collected sediment cores, grab samples, current velocity data using an acoustic Doppler current profiler (ADCP), and high-resolution bathymetry data using a multibeam echosounder. Bathymetric data show that the subaqueous delta front has a well-developed submarine channel which is fed by numerous gullies originating at the fjord walls and delta lip. The proximal channel is ~170 m in width, and here the channel bed is comprised of coarse- and medium-grained sand, organized into crescent-shaped scours and bedforms (25 m wavelength, 1 m in height) in the thalweg. The distal part of the channel widens toward the basin (~450 m), and the relief of channel flanks decreases from the delta lip to deep water. Distal bedforms consist of fine sand, likely due to the slope transition from the delta front to the basin floor of the fjord reducing sediment transport capacity. ADCP data at the proximal delta front demonstrate that near-bed bottom currents reach up to 1.6 m/s and the thickness of the measured flow is up to 10 m. This research demonstrates that turbidity currents, which can efficiently transport sediment from the subaerial delta to deep water, occur under normal meltwater pulse discharge conditions and influence the delta-front morphology of the Quinnguata Kuussua river.

Sarah Garcia

Carbon Emission as a Consequence of High Sedimentation and Drought at Elephant Butte Reservoir, New Mexico

The Western United States experiences extreme droughts, which necessitates the construction of reservoirs for agricultural, recreational, and municipal use. However, these reservoirs lose more than 2% of their capacity to contain water every year due to high sedimentation rates, driven by the sparse vegetation and easily erodible sediment characteristic of semiarid environments. Alongside sediment, organic matter is sequestered in reservoirs. Inland waters, including reservoirs, cover less than 2% of Earth's surface and bury ~0.15 PgC/year, approaching the rate of carbon burial of oceans, which is ~0.20PgC/year. Here, this study evaluates sediment accumulation and carbon sequestration at Elephant Butte Reservoir (EBR), which rests on the Rio Grande River in New Mexico. EBR exhibits rapid sedimentation driven by annual monsoon flooding and spring snowmelt. As sediment accumulates within the reservoir, organic matter is also sequestered, allowing the reservoir to operate as an organic carbon sink. Where the Rio Grande meets the reservoir, it builds a delta that experiences regular base-level fluctuations in response to the reservoir water level, which is often impacted by drought conditions. During high water level, sediment and organic matter is deposited on the delta by overbank sedimentation and through the formation of hyperpycnal plumes. During low base-level conditions, the delta top is exposed to the atmosphere, and the sediment and carbon that was deposited on the delta top may be disturbed. Depending on the burial depth and degree of sediment disturbance, organic material may be exposed to the atmosphere and release CO2. We evaluate the potential for carbon release at EBR through remote sensing and field observation. We visualize the frequency and periodicity of inundation within EBR by building wetted frequency maps, derived from applying the Normalized Difference Water Index to images obtained from Landsat 4, 5, 7 and 8. We use the wetted frequency maps to inform sediment sample locations, which are subjected to loss on ignition (LOI) to determine carbon content. We expect that carbon content will correlate with wetted frequency wherein a less inundated sampling area is expected to coincide with less carbon content in the sample. Vegetation density and species are also documented during field campaigns to assess root structures, and thus length scales of sediment reworking by plants. We also excavate trenches, up to 60 cm deep, to observe the shallow deltaic stratigraphy and to understand carbon distribution in the shallow subsurface. Understanding the impacts that inland reservoirs have on regional organic carbon is important to fully interpret its effects on the global carbon cycle.

The Student Body Committee

Arya Tilak - Student Research Conference Chair

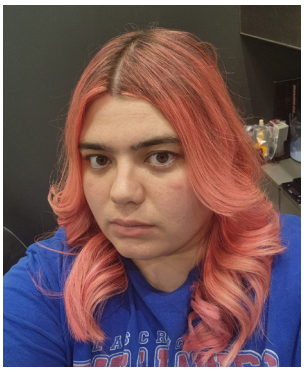

Karissa Vermillion - Geology Representative

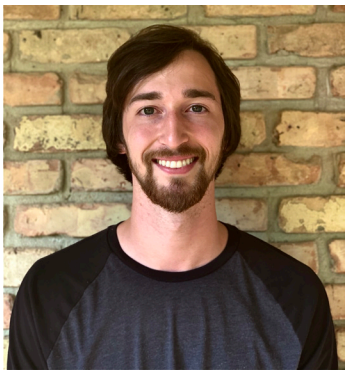

Joe McNease - Geophysics Representative

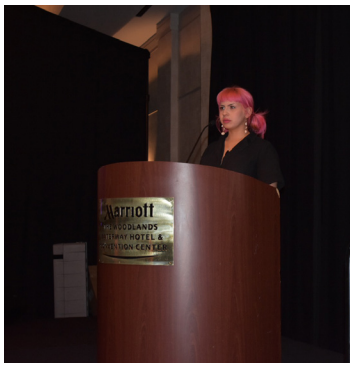

Morgann Farley - Undergrad Representative

Shannon Dixon - Undergrad Representative

Thank you to all of the volunteer faculty and industry judges. This would not have been possible without you!

Brandee Carlson
Adam Goss
Chukwudi Anene
Bernhard Rappenglueck
Jinny Sisson
Julia Wellner
Dan Hauptvogel
Minako Righter
Jagos Radovic
Xun Jiang

Sophie Broun
Jon Rotzien
Brian Horn
Antonio Nocioni
Ceri Davies
Jose Gorosabel
Eric Williams
Luke Walker
Juliet Irvin
Evgeny Chesnokov

We would also like to thank and acknowledge the College of Natural Science and Mathematics for their contributions to the 2024 Student Research Conference. Thank you for your support!

UNIVERSITY OF HOUSTON

COLLEGE OF NATURAL SCIENCE AND MATHEMATICS

Who Are We?

The Department of Earth and Atmospheric Sciences at the University of Houston has a wide range of research programs central to the earth sciences.

Air Pollution
Air Quality
Applied Geophysics
Applied Rock Physics
Atmospheric Science
Carbonate Petrology
Climatology
Geodynamics
GIS
Hydrology
Igneous Petrology
Inorganic Geochemistry
Isotope Geochemistry
Marine Geology
Micropaleontology
Potential Fields
Remote Sensing
Sedimentology
Seismology
Sequence Stratigraphy
Structural Geology
Tectonics
Thermochronology
Whole Earth Geophysics

The Department offers M.S. and Ph.D. degrees in Geology, Geophysics, and Atmospheric Sciences, a B.S. in Geology, Geophysics, and Environmental Sciences, and a B.A. in Earth Sciences. Fieldwork is a major component of all degree programs. The Department also offers Professional M.S. programs in Petroleum Geology and Petroleum Geophysics that are offered at convenient hours for professional geoscientists working in industry or aspiring for a professional position within the petroleum industry.

CONTACT US

Department of Earth and Atmospheric Science
4800 Cullen Boulevard, Houston, Tx 77204
Phone: (713) 743-3399
Web: http://www.eas.uh.edu